Comparison of Iron Loss Models for Electrical Machines With Different Frequency Domain and Time Domain Methods for Excess Loss Prediction

Damian Kowal[1], Peter Sergeant[1,2], Luc Dupré[1], and Lode Vandenbossche[3]

[1]Department of Electrical Energy, Systems and Automation, Ghent University, Gent B-9000, Belgium
[2]Department of Industrial Technology and Construction, Ghent University, Gent B-9000, Belgium
[3]ArcelorMittal Global Research and Development Gent, Zelzate B-9060, Belgium

The goal of this paper is to investigate the accuracy of modeling the excess loss in electrical steels using a time domain model with Bertotti's loss model parameters n_0 and V_0 fitted in the frequency domain. Three variants of iron loss models based on Bertotti's theory are compared for the prediction of iron losses under sinusoidal and non-sinusoidal flux conditions. The non-sinusoidal waveforms are based on the realistic time variation of the magnetic induction in the stator core of an electrical machine, obtained from a finite element-based machine model.

Index Terms—**Electrical steel, excess losses, iron losses, loss modeling.**

I. Introduction

A GENERAL approach for the calculation of iron loss in soft magnetic laminated materials under a unidirectional flux $\phi(t)$ is based on the separation of the losses into three components: 1) the hysteresis loss P_h; 2) the classical loss P_c; and 3) the excess loss P_e [1]. The statistical loss theory under arbitrary flux waveforms and no minor loops is described in [2], whereas [3] takes into account the minor order loops. Here, we may distinguish between frequency and time domain loss models.

Both frequency and time domain loss models require the identification of certain material-dependent parameters. For the identification of the hysteresis loss P_h, quasi-static measurements of iron loss are carried out. In the case of modeling the classical loss P_c, when neglecting skin effect, the electrical steel sheet-dependent parameters are the lamination thickness d and electrical conductivity σ. Both parameters are easily measured.

In [4], the microstructural-dependent parameters describing the excess loss component P_e are defined as n_0 and V_0. Both parameters can be fitted in the frequency and time domain on the basis of iron loss measurements for a range of frequencies and peak induction values. The fitting method in the frequency domain can be found in [5] and is later described in this paper. It is shown how significant is the error introduced using the material parameters fitted in the frequency domain to estimate the losses in the time domain model.

The iron loss models, both frequency and time domain, exist with different levels of complexity. In this paper, we compare the loss prediction of three models with different complexity, i.e., two frequency domain models and one time domain model. The accuracy of these three different models is tested both for sinusoidal and non-sinusoidal flux waveforms. A set of iron loss measurements was performed with an Epstein frame for both kinds of waveforms. The considered material is a fully processed non-oriented thin laminated, highly alloyed, low loss steel grade with a large grain size, and therefore, with a high excess loss component. Indeed, the total iron loss (for a time-dependent applied magnetic field) contains three components: 1) hysteresis loss; 2) classical eddy current loss; and 3) excess loss. The hysteresis loss may be measured by applying the same waveform for the magnetic field but at a frequency going in the limit to 0 Hz and consequently no dynamic effects are present. The classical loss component is computed from the formulas obtained from Maxwell's equations and assuming a linear relation between the magnetic induction and magnetic field. The excess loss is measured (segregated) by subtracting from the measured total iron loss, the hysteresis and classical loss component, the last two obtained as described in the previous sentences.

The choice of the non-sinusoidal flux waveforms is related to the estimation of the iron loss in electrical machines. Indeed, the magnetic induction waveforms in the stator teeth and yoke are non-sinusoidal, due to slot effects and non-sinusoidal currents in the copper windings [6], [7]. It is investigated how significant the loss error becomes by taking a simple frequency domain model based on the peak value of the full waveform. This paper investigates also the error introduced using material related loss parameters identified from sinusoidal waveform measurements when the losses are estimated for a non-sinusoidal waveform.

Manuscript received February 6, 2014; revised May 19, 2014; accepted June 19, 2014. Date of publication July 11, 2014; date of current version January 26, 2015. Corresponding author: D. Kowal (e-mail: damian.a.kowal@gmail.com).

Color versions of one or more of the figures in this paper are available online at http://ieeexplore.ieee.org.

Digital Object Identifier 10.1109/TMAG.2014.2338836

II. Theoretical Analysis

A. Statistical Loss Theory for Unidirectional Time Periodical Flux Conditions

It is well known that the dynamic losses, i.e., the classical and excess losses are the result of induced electrical

currents due to the time varying magnetic flux appearing in the electrical steel. According to the classical theory, where the material is assumed to be magnetized in a homogeneous way, these induced electrical currents are also distributed in a homogeneous way, as described by Maxwell's equations. Due to the magnetic domain structure in electrical steels, these induced electrical currents are not varying in a homogeneous way in space but are located around moving magnetic domain walls. One can attempt a general phenomenological description of the magnetization process, where a certain number n of active correlation regions, randomly distributed in the specimen cross section, produce the overall observed magnetic flux variation $\phi(t)$ [1]. Correlation regions are a way to describe the fact that, given a Barkhausen jump, there is an enhanced probability that the next jump will take place in the neighborhood of the previous one. The term magnetic objects is often used in the literature to refer to these correlation regions containing strongly interacting magnetic domain walls. Notice that $\phi(t)$ in this paper is defined as the flux in a 1 m wide lamination with thickness d.

The applied magnetic field $H_s(t)$ (magnetic field at the surface of the electrical steel sheet with lamination thickness d) corresponding with the magnetic flux density $B(t)$ in the electrical steel sheet has a hysteresis, a classical, and an excess field component, denoted by $H_h(t)$, $H_c(t)$, and $H_e(t)$, respectively. Then, the instantaneous hysteresis, classical, and excess loss components can be written as

$$p_h(t) = H_h(t)\frac{dB}{dt},\ p_c(t) = H_c(t)\frac{dB}{dt},\ p_e(t) = H_e(t)\frac{dB}{dt} \quad (1)$$

$$B(t) = \frac{\phi(t)}{d} = \frac{1}{d}\int_{-d/2}^{d/2} B_l(x,t)dx \quad (2)$$

and

$$P_h = \frac{1}{T_p}\int_0^{T_p} p_h(t)dt \quad (3)$$

$$P_c = \frac{1}{T_p}\int_0^{T_p} p_c(t)dt \quad (4)$$

$$P_e = \frac{1}{T_p}\int_0^{T_p} p_e(t)dt \quad (5)$$

where $B_l(x,t)$, d, and T_p are local magnetic induction in the sheet, thickness of the sheet, and period of the applied magnetic field $H_s(t)$, respectively. The instantaneous classical loss $p_c(t)$ is given by [1]

$$p_c(t) = \frac{\sigma d^2}{12}\left(\frac{dB}{dt}\right)^2. \quad (6)$$

In addition, for the instantaneous excess loss $p_e(t)$, equations can be derived from Bertotti's theory. When focussing on the excess field $H_e(t)$, it is shown in [1] that this field can be written as a function of electrical conductivity σ, the cross section of the electrical sheet S, and the time derivative of the magnetic flux density in the electrical sheet

$$H_e(t) = \frac{\sigma \mathrm{GS}}{n(t)}\left(\frac{dB}{dt}\right). \quad (7)$$

Notice that the number of simultaneously reversing magnetic objects n may vary in time and G is a dimensionless coefficient [2]

$$G = \frac{4}{\pi^3}\sum_k \frac{1}{(2k+1)^3} = 0.1356\ldots \quad (8)$$

The two time-dependent functions in (7), i.e., $H_e(t)$ and $n(t)$, are not independent. In the statistical loss theory of Bertotti, simple relations between them are postulated and the resulting excess loss equations are then validated experimentally. From electromagnetic loss measurements, it became clear that the assumption

$$n(t) = n_0 + \frac{H_e(t)}{V_0} \quad (9)$$

holds quite well for the magnetization processes under unidirectional magnetic fields for non-oriented electrical steels and rolling direction of grain-oriented electrical steels. The material behavior under rotational field conditions is out of the scope of this paper.

From (7) and (9), one obtains for an increasing magnetic flux density, by eliminating $n(t)$

$$H_e(t) = \frac{1}{2}\left(\sqrt{n_0^2V_0^2 + 4\sigma \mathrm{GS}V_0\frac{dB}{dt}} - n_0V_0\right) \quad (10)$$

and consequently from (1)

$$p_e(t) = \frac{1}{2}\left(\sqrt{n_0^2V_0^2 + 4\sigma \mathrm{GS}V_0\frac{dB}{dt}} - n_0V_0\right)\frac{dB}{dt}. \quad (11)$$

From (5), (6), and (11), one may compute the classical and excess loss for any arbitrary time-dependent periodic magnetic flux pattern

$$P_c = \frac{\sigma d^2}{12}\frac{1}{T_p}\int_0^{T_p}\left(\frac{dB}{dt}\right)^2 dt \quad (12)$$

and

$$P_e = \frac{1}{T_p}\int_0^{T_p}\frac{1}{2}\left(\sqrt{n_0^2V_0^2 + 4\sigma \mathrm{GS}V_0\left|\frac{dB}{dt}\right|} - n_0V_0\right)\left|\frac{dB}{dt}\right| dt. \quad (13)$$

The material parameters n_0 and V_0 can be derived from electromagnetic loss measurements—often under sinusoidal magnetic flux conditions—at different frequencies and induction levels as follows.

The total iron loss can then be calculated as

$$P_t = P_h + P_c + P_e. \quad (14)$$

B. Statistical Loss Theory Under Sinusoidal Flux Patterns

In this case, a sinusoidal unidirectional flux $\phi(t) = dB_p\sin(2\pi ft)$ or a period unidirectional flux without local minima or maxima is enforced to the electrical steel sheet no local minima in the induction waveform will appear (absence of minor hysteresis loops). Therefore, it can be assumed that hysteresis loss is only related to the peak value B_p. If $W_h(B_p)$

defines hysteresis energy loss per cycle for a given B_p, then the hysteresis power loss can be expressed as

$$P_h = W_h(B_p) f. \tag{15}$$

Moreover, when the skin effects may be neglected, then for the sinusoidal flux (12) reduces to

$$P_c = \frac{1}{6}\sigma \pi^2 d^2 B_p^2 f^2. \tag{16}$$

According to the statistical loss theory [1], the magnetization process for an arbitrary periodic magnetic flux $\phi(t)$ in a given cross section S of the lamination can be described in terms of a number of *n(t)* simultaneously active correlation regions, given by, see also (7)

$$n(t) = \frac{\sigma \mathrm{GS}\left(\frac{dB}{dt}\right)^2}{H_e(t)\frac{dB}{dt}}. \tag{17}$$

One may approximate the time average of $n(t)$ by

$$\tilde{n} = < n > \approx \frac{\frac{1}{T_p}\int_0^{T_p} \sigma \mathrm{GS}\left(\frac{dB}{dt}\right)^2 dt}{\frac{1}{T_p}\int_0^{T_p} H_e(t)\frac{dB}{dt} dt} = \frac{\frac{1}{T_p}\int_0^{T_p} \sigma \mathrm{GS}\left(\frac{dB}{dt}\right)^2 dt}{P_e}. \tag{18}$$

In the case of a piecewise linear time variation of $B(t)$ with only an absolute maximum and minimum, (18) becomes

$$\tilde{n} = < n > = \frac{16\sigma \mathrm{GS} B_p^2 f^2}{P_e} \tag{19}$$

while in the case of a sinusoidal flux, one has

$$\tilde{n} = < n > \approx \frac{2\pi^2 \sigma \mathrm{GS} B_p^2 f^2}{P_e}. \tag{20}$$

When defining the time averaged excess field $\tilde{H}_e$ by

$$\tilde{H}_e = \frac{P_e}{4 B_p f} \tag{21}$$

we may rewrite (9) as

$$\tilde{n} = n_0 + \frac{\tilde{H}_e}{V_0}. \tag{22}$$

Combining (19), (20), and (22), we obtain for the excess loss under a piecewise linear time variation of $B(t)$ with only an absolute maximum and minimum

$$P_e = 2 B_p f \left(\sqrt{n_0^2 V_0^2 + 16\sigma \mathrm{GS} V_0 B_p f} - n_0 V_0\right) \tag{23}$$

and under a sinusoidal flux pattern

$$P_e = 2 B_p f \left(\sqrt{n_0^2 V_0^2 + 2\pi^2 \sigma \mathrm{GS} V_0 B_p f} - n_0 V_0\right). \tag{24}$$

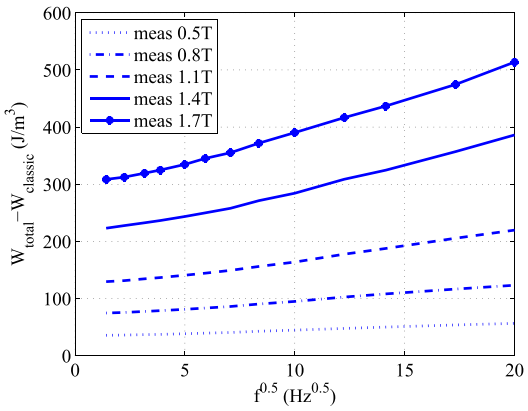

Fig. 1. Measured total loss minus classical loss versus square root of frequency. Energy loss is given per unit volume.

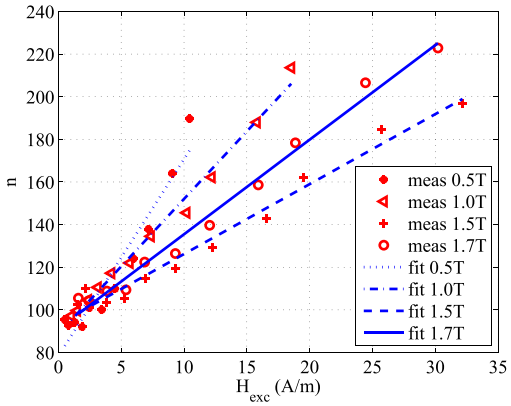

Fig. 2. Number of active correlation regions under sinusoidal flux conditions.

C. Identification of n_0 and V_0 Using the Frequency Domain Approach

The identification of the microstructural-dependent parameters n_0 and V_0 is based on electromagnetic loss measurement under sinusoidal flux for different frequencies and peak induction values.

By subtracting from the measured total loss $P_{t,m}(B_p, f)$ (W/m^3) the classical loss $P_c(B_p, f)$ given by (16), we may construct $(P_h + P_e)/f$ as a function of the square root of the frequency f for the considered frequencies and induction peak levels (Fig. 1). By extrapolating the functions to zero frequency, we may identify the measured hysteresis loss $P_{h,m}(B_p)$ (W/m^3) and consequently also the measured excess loss $P_{e,m}(B_p, f) = P_{t,m}(B_p, f) - P_c(B_p, f) - P_{h,m}(B_p)$.

In a next step, we construct the function values $\tilde{n}(\tilde{H}_e)$ for discrete values of B_p and f. Here, we make use of (20) and (21), see Fig. 2

$$\tilde{n} = \frac{2\pi^2 \sigma \mathrm{GS} B_p^2 f^2}{P_{e,m}} \tag{25}$$

and

$$\tilde{H}_e = \frac{P_{e,m}}{4 B_p f}. \tag{26}$$

Notice that in Fig. 2, data is used up to 400 Hz. At this frequency, the considered electrical steel with a resistivity of

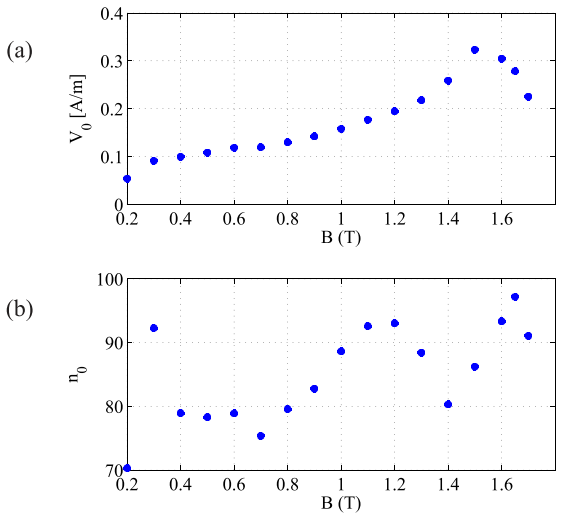

Fig. 3. n_0 and V_0 fitted from measurements as a function of B_p.

60 $\mu\Omega\cdot$cm and maximum relative permeability of 5420, has a skin depth ~0.265 mm, which is significantly more than half of the thickness, i.e., 0.15 mm of the steel sheet. Consequently, skin effects may be assumed to be negligible for the data used to identify the material properties in the different models.

The parameters n_0 and V_0 are then identified by constructing the linear function $\tilde{n}(\tilde{H}_e)$ approximating the discrete function values for the different B_p values (Fig. 2). The values for n_0 and V_0 are given in Fig. 3. n_0 and V_0 are parameters depending on the cross section S of the lamination, but show also a B_p-dependence.

Notice that in literature, for the construction of the $\tilde{n}(\tilde{H}_e)$ functions, not (20) but (19) is used even with measurement data under sinusoidal flux conditions. As such, this is not a problem as long as the parameter values, identified using the excess loss equations in the frequency domain, for n_0 and V_0 are later on used for the loss evaluation using the same frequency domain equation, i.e., (23). Inaccuracies may occur when using the parameter values in the expressions in the time domain, i.e., (13). The issue of using n_0 and V_0 fitted in the frequency domain with (19) or (20) for the excess loss estimation in the time domain is studied in detail in Section IV-D.

III. Loss Models Used for Comparison

For the comparison, three loss models are used. Two of them are frequency domain models, which means that they assume sinusoidal waveforms of the magnetic induction with peak value B_p. The third model is a time domain model, which is suitable for performing loss predictions for an arbitrary flux waveform, where no minor loops are included.

A. Frequency Domain Model (Model 1)

For the calculation of the classical loss component, (16) is used with the values of d and σ corresponding with the investigated steel grade.

The first version of the frequency domain model is using (15) for the hysteresis loss calculation. The $W_h(B_p)$ is obtained by loss measurements performed on the Epstein frame at 2 Hz (quasi-static) and a range of peak induction values. It is assumed that the dynamic losses for the considered frequency are negligible. Therefore, the classical and excess losses are not considered. The value of $W_h(B_p)$ for a random B_p is identified by interpolation using the values obtained from the measurements.

Finally, the excess loss component is calculated with (24) for the sinusoidal flux conditions. The parameters n_0 and V_0 are fitted based on loss measurements as presented in Section II-C. Notice that parameters n_0 and V_0 are dependent on the peak value B_p of the magnetic induction.

B. Simplified Frequency Domain Model (Model 2)

The second-frequency domain model is a simplified version of model 1. The following equation is used for the total iron loss calculation:

$$P_{\text{tot}} = P_h + P_c + P_e = aB_p^{\alpha} f + bB_p^2 f^2 + cB_p f\left(\sqrt{1+eB_p f}-1\right) \quad (27)$$

where α, a, b, c, and e are material related parameters fitted based on the loss measurements under sinusoidal flux condition. The procedure of fitting the parameters is as follows. First, the b parameter is calculated based on (16). Second, the parameters α and a are fitted for the curve $W_h(B_p)$ that is obtained in the same way as in model 1. Finally, the excess losses segregated from the measurements are calculated for the whole range of B_p and frequencies as: $P_e = P_{\text{tot}} - P_h - P_c$. Then, the parameters c and e are fitted to correspond with the calculated excess losses P_e. It is important to know that—in contrast with model 1—c and e are independent from B_p. For the fitting procedure, the least square method is used.

C. Time Domain Model (Model 3)

The third model is the time domain model that is suitable to use for iron loss calculation for an arbitrary flux waveform without minor loops. The hysteresis losses are calculated as in the first frequency domain model (15). The classical losses are calculated considering (12), where the excess loss is quantified by (13). For the excess loss equation, the parameters n_0 and V_0 are fitted in the frequency domain as presented in Section II-C. Notice that n_0 and V_0 are again functions of B_p (Fig. 3).

IV. Numerical Validation of the Time and Frequency Electromagnetic Loss Models for Sinusoidal Flux Waveforms

For the comparison of the different iron loss models, a fully processed non-oriented electrical steel of 0.3 mm thickness was selected, with a high ratio of excess to total loss. For the selected steel grade, a set of measurements under a sinusoidal flux was performed for 13 frequencies in the range from 2 to 400 Hz and for 16 peak induction values between 0.2 and 1.7 T. Table I presents the three segregated loss components, measured at a 1.5 T peak induction value and frequencies of 50 and 400 Hz. Notice that for 50 Hz, the

TABLE I
THREE IRON LOSS COMPONENTS SEGREGATED FROM LOSSES MEASURED FOR 1.5 T AND A FREQUENCY OF 50 AND 400 Hz UNDER SINUSOIDAL FLUX CONDITION (W/kg)

	hysteresis losses	classical losses	excess losses	total losses
50 Hz	1.743	0.178	0.264	2.185
400 Hz	13.943	11.412	10.242	35.597

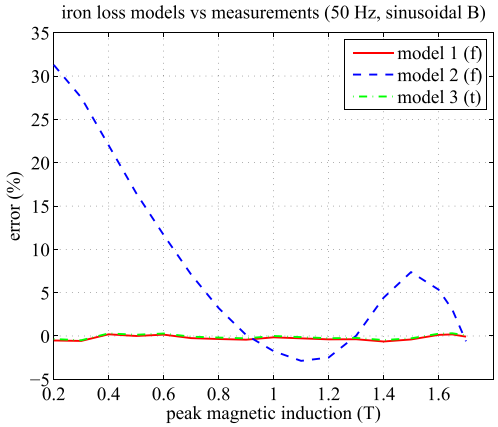

Fig. 4. Error between the iron loss value estimated by the three loss models and measured value of losses for 50 Hz frequency as a function of the peak magnetic induction value of the sinusoidal magnetic induction waveform.

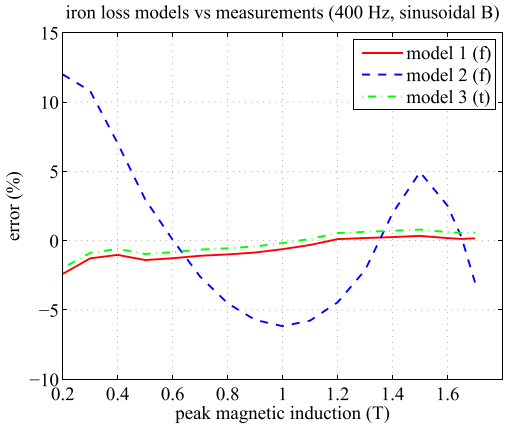

Fig. 5. Error between the iron loss value estimated by the three loss models and the measured value of losses for 400 Hz frequency as a function of the peak magnetic induction value of the sinusoidal magnetic induction waveform.

hysteresis loss is dominant, whereas for 400 Hz, all three components of loss are of the same order.

Based on the iron loss measurements under sinusoidal flux conditions, the fitting of the loss model parameters is performed (Section III). The models are then used to estimate the iron losses for the created sinusoidal magnetic induction waveform with the frequency of 50 and 400 Hz. The results of the iron loss estimation are compared with the measured values.

Figs. 4 and 5 present the error between the estimated and measured total iron loss values. It can be observed that the more complex frequency domain model (model 1) and time domain model (model 3) correspond very well with the

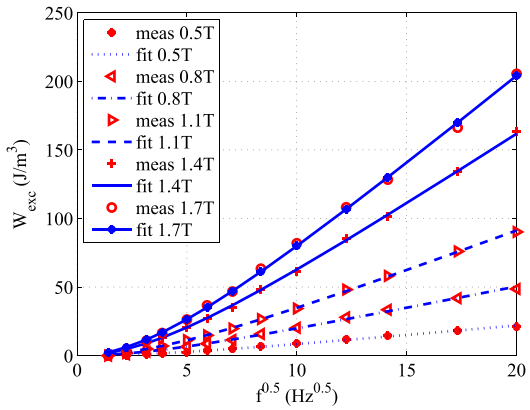

Fig. 6. Simulated and segregated from measurements excess losses under sinusoidal magnetic induction for several values of the peak magnetic induction. Simulation of excess losses in the frequency domain with n_0 and V_0 fitted in the frequency domain as used by model 1. Exact values of n_0 and V_0 as presented in Fig. 3 are used in the simulation.

measurements under sinusoidal flux condition. Both models have a very similar low-level error. The errors of these two models are higher for the case of 400 Hz. In addition, the difference in error between models 1 and 3 is also higher for higher frequency. This is because for 400 Hz, the excess loss component is more significant (Table I) and the discrepancy between the two models is mainly in the estimation of this loss component. As it is expected, model 2 has a much higher error for all frequencies when compared with the other two models. This is due to the less accurate calculation method of hysteresis and excess loss components (B_p independent material parameters).

For a better understanding of the difference between loss models 1 and 3, it is necessary to compare how they estimate the excess loss, since both models under sinusoidal flux condition will result in the same value for the hysteresis and classical loss components.

A. Excess Loss Calculation in the Frequency Domain for a Sinusoidal Flux Waveform (Model 1)

For the n_0 and V_0 fitted as presented in Fig. 3, the excess losses were calculated to validate the loss model. Notice that the fitting of the material parameters was performed with (25) corresponding with the sinusoidal flux waveform. The loss model using (24) for the excess loss calculation is using sinusoidal waveforms that have corresponding peak induction values and frequencies with the measured data. Simulated and measured data are compared.

First, to predict the excess losses for a sinusoidal waveform and given B_p, the exact values of n_0 and V_0 as in Fig. 3 were used in (24), resulting in Fig. 6. It can be observed that the calculated excess losses are corresponding very well with the segregated ones, which confirms a good fitting of the parameters n_0 and V_0. Fig. 7 presents the error in excess loss estimation between segregation results and frequency domain loss model (model 1). The average value of the error for the considered range of frequencies and peak magnetic induction values equals 3.2%.

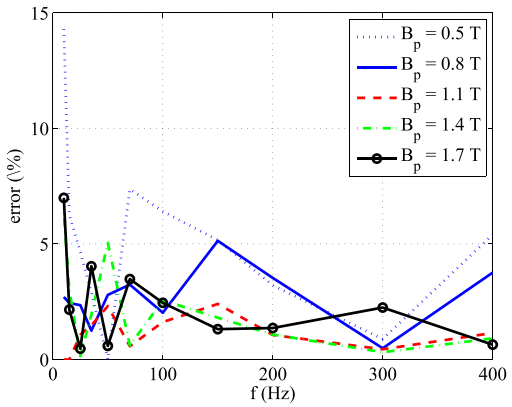

Fig. 7. Error in the estimation of the excess losses by the frequency domain model with the use of parameters n_0 and V_0 fitted for frequency domain equation. Values of parameters presented in Fig. 3.

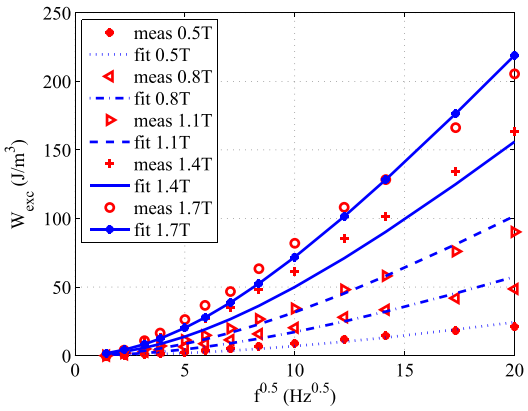

Fig. 8. Simulated and segregated from measurements excess losses under sinusoidal magnetic induction for several values of the peak magnetic induction. Simulation of excess losses in the simplified frequency domain model (model 2).

The second step is the error analysis, when approximating the $n_0(B_p)$ and $V_0(B_p)$ functions by constant functions $n_0 = 85.125$ and $V_0 = 0.177$ [A/m]. This leads to constant excess loss coefficients, similar to model 2. This approximation introduces additional errors, especially in the range of higher B_p value and higher frequencies. The average value of the error is equal to 7.5%.

Finally, functions $n_0(B_P)$ and $V_0(B_p)$ are approximated by linear functions: 1) $V_0 = 0.153B_p + 0.025$ [A/m] and 2) $n_0 = 10.248B_p + 74.968$. Since the linear function follows better the B_p dependence of n_0 and V_0 than a constant, the average error drops to 5.2%.

It can be concluded that the exact values of n_0 and V_0 obtained from the fitting procedure give the lowest error in excess loss prediction. In addition, the better the approximation function corresponds with the B_p dependence of n_0 and V_0, the lower the error of the predicted losses compared with the segregated excess losses.

B. Excess Loss Calculation in the Frequency Domain for Sinusoidal Flux Waveform (Model 2)

The estimation of the excess losses in the simplified frequency domain model is based on

$$P_e = cB_b f\left(\sqrt{1 + eB_p f} - 1\right) \tag{28}$$

where the parameters c and e are fitted with a least square method based on the loss measurements. Notice that the obtained parameters are B_p independent.

Fig. 8 shows the predicted values of the excess losses in comparison with the segregated ones for a range of frequencies and few values of the peak magnetic induction. By comparing Fig. 8 with Fig. 6, it is clear that the simplified model 2 has much less accuracy in predicting the excess losses. This is also confirmed by Fig. 9, which shows the error that model 2 introduces with respect to loss segregation results. The average error introduced by model 2 is 19.3%. Notice that the correspondence between predicted and segregated excess losses is at its best for the middle range of frequencies, which in this case is ~200 Hz (Fig. 9).

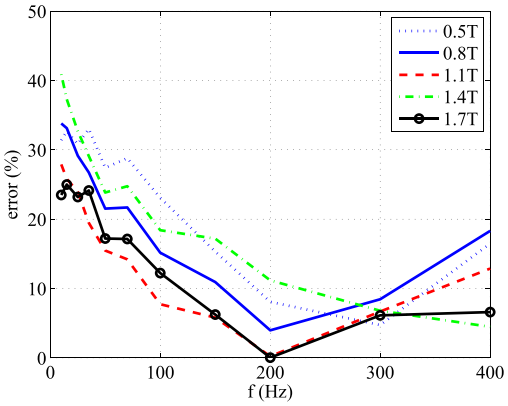

Fig. 9. Error in the estimation of the excess losses by the simplified frequency domain model (model 2).

C. Excess Loss Calculation in the Time Domain for a Sinusoidal Flux Waveform and n_0 and V_0 Fitted Based on (25) (Model 3)

In the time domain model, the excess losses are calculated with the same n_0 and V_0 as in the frequency domain model (model 1). This means that for the fitting of the parameters, (25) was used while for the excess loss prediction, we considered (13). Fig. 10 presents the comparison of the segregated excess losses with the excess losses calculated by the loss model with the use of the time domain equations. The dependence on the peak magnetic induction of the parameters n_0 and V_0 used in Fig. 10 is exactly as in Fig. 3. Fig. 11 presents the error in excess loss estimation between segregation and loss model (13). The average error in excess loss prediction is equal to 3.5%. This can be compared with the error introduced by the frequency domain model 1 that equals 3.2%. It is clear that for a sinusoidal flux the n_0 and V_0 parameters fitted in the frequency domain model with (25) can be used for the prediction of the excess losses in the time domain model without introducing significant errors.

Similar as in the case of model 1, when the B_p dependence of n_0 and V_0 is approximated by a constant, the average value of the error increases to 7.4%. When introducing in

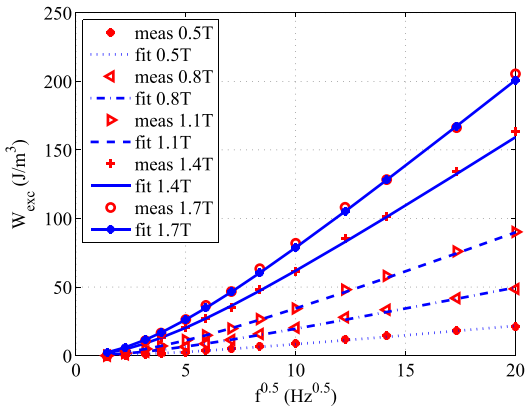

Fig. 10. Simulated and segregated from measurements excess losses under sinusoidal magnetic induction for several values of the peak magnetic induction. Simulation of excess losses in time domain with n_0 and V_0 fitted in the frequency domain. Exact values of n_0 and V_0 as presented in Fig. 3 are used in the simulation.

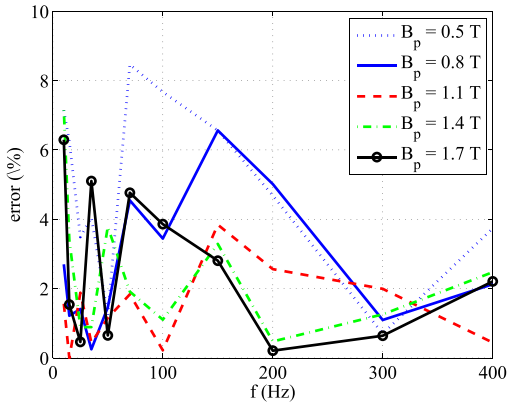

Fig. 11. Error in the estimation of the excess losses in time domain with the use of parameters n_0 and V_0 fitted for frequency domain equation. Values of parameters presented in Fig. 3.

model 3 the same linear dependence of $n_0(B_P)$ and $V_0(B_p)$ as in model 1, the average error of the computed excess loss with respect to the segregation results equals 5.1%.

D. Excess Loss Calculation in the Time Domain With n_0 and V_0 Fitted in the Frequency Domain With (19)

Until now, the n_0 and V_0 parameters used in the time domain model were fitted with (25) in the frequency domain. Based on the comparison of Figs. 7 and 11, it can be concluded that this approach does not introduce significant errors. In addition, the equation commonly used in literature for the fitting of n_0 and V_0 in the frequency domain starting from measurements under sinusoidal flux patterns is (19) instead of (20) [8], [9]. We recall that (19) was derived when assuming a piecewise linear time variation of $B(t)$.

It is interesting to know what kind of error is introduced when the n_0 and V_0 fitted with (19) are used in the time domain model.

Fig. 12 presents the error between the estimated loss values and the ones segregated from measurements, for the time domain model, where the n_0 and V_0 parameters are fitted

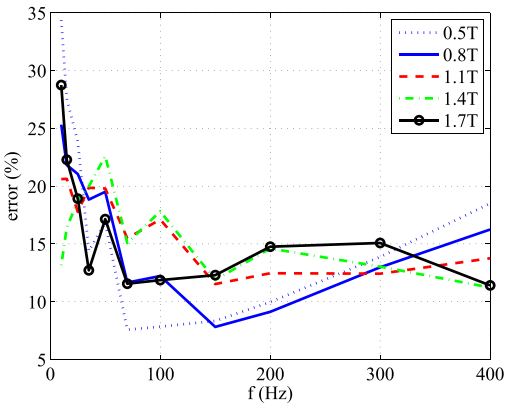

Fig. 12. Error in the estimation of the excess loss in time domain with the use of parameters n_0 and V_0 fitted for frequency domain equation with (19) for piecewise linear flux used for fitting.

in frequency domain with (19). The average value of the error for the whole range of frequency and B_p values equals 19.3%. This means that the often used approach for identifying n_0 and V_0 and later on used in a time domain model, introduces a 16% higher error than the approach presented in Section II-C and Fig. 7.

V. Numerical Validation of the Time and Frequency Domain Iron Loss Models for Non-Sinusoidal Flux Waveforms

In Section IV, it is shown how three loss models correspond with measurements when a sinusoidal flux variation is considered. However, loss models are often used to predict iron losses in electromagnetic devices, for example, in electrical machines [10], [11]. It is known that the flux variation in different parts of the core of the electrical machines might be non-sinusoidal. Here, the accuracy of loss prediction of all three models for a set of non-sinusoidal magnetic induction waveforms is presented. For all considered waveforms, the iron losses were measured on the Epstein frame.

The frequency domain model 1 calculates the hysteresis losses based on the maximum induction value $B_{\max}$ of the complete waveform. To improve the accuracy of model 1 for a non-sinusoidal flux, a Fourier analysis of the waveforms is performed and dynamic losses (classical and excess) are calculated for each of the harmonics with the respective B_i value, where B_i is the peak value of harmonic i. For each harmonic i, the value of n_0 and V_0 corresponds with B_i. The total dynamic loss is obtained by summing up the contributions of all considered harmonics. Notice that the excess loss component will also depend on the phase shift between harmonics. Therefore, the approach used in model 1 for distorted induction waveform is only an approximation.

The second frequency model (model 2) calculates the losses only for the $B_{\max}$, as the waveform would be a sinusoidal one with given f and $B_p = B_{\max}$.

The time domain model (model 3) does not need any adjustments for the non-sinusoidal waveform. The value of n_0 and V_0 corresponds with $B_{\max}$.

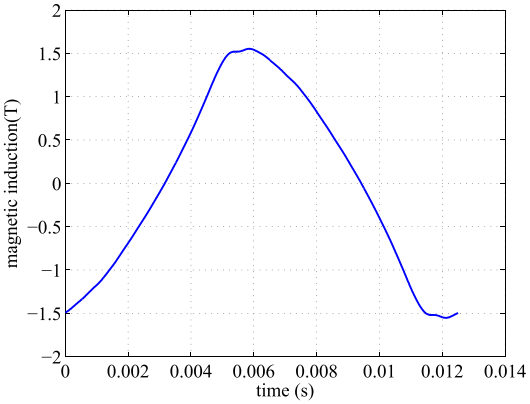

(a)

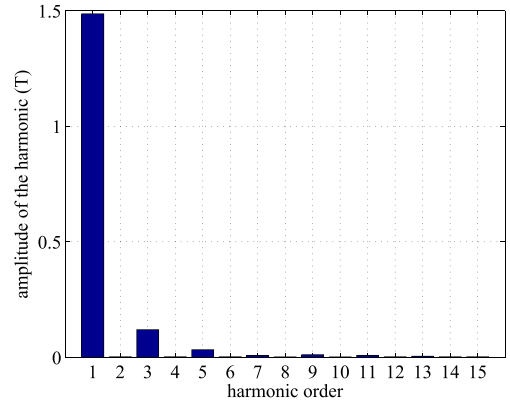

(b)

Fig. 13. (a) Magnetic induction waveform recorded in the stator yoke of the low frequency machine (80 Hz). Simulation time is one electrical period of the machine. (b) Harmonic content of the waveform.

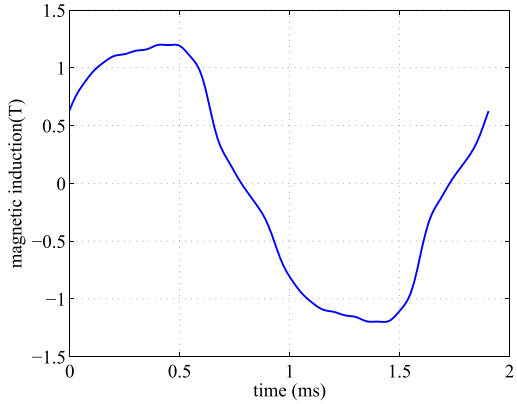

(a)

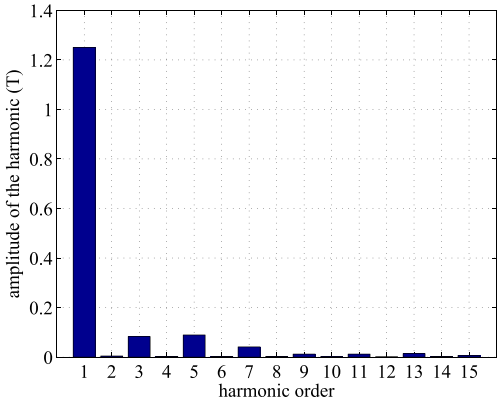

(b)

Fig. 14. (a) Magnetic induction waveform recorded in stator core of the high-frequency machine (525 Hz, $B_{\max} = 1.2$ T). Simulation time is one electrical period of the machine. (b) Harmonic content of the waveform.

TABLE II

LOSS VALUES ESTIMATED BY THE THREE LOSS MODELS FOR THE LOW-FREQUENCY WAVEFORM RECORDED IN THE STATOR YOKE OF THE LOW-FREQUENCY MACHINE AND CORRESPONDING ERROR TO THE MEASURED VALUE, AND LOSSES IN W/kg

	model 1 (frequency)		model 2 (frequency)	model 3 (time)
tot. loss	4.107*	4.117	3.827	4.095
hyst. loss	2.958*	2.958	2.814	2.958
class. loss	0.489*	0.487	0.489	0.487
exc. loss	0.660*	0.672	0.524	0.650
error	3.70%*	3.47%	10.28%	3.99%

* losses calculated for fundamental f, where $B_p = B_{max}$.

Notice that all the material parameters for the iron loss models are fitted based on the measurements performed for a sinusoidal flux.

For the validation and comparison of the models, the non-sinusoidal flux waveforms come from the finite element (FE) simulations of two electrical machines. The FE simulations were performed with COMSOL. The magnetic induction values were recorded in certain points of the machine geometry. The time variation of magnetic induction was recorded for one electrical period of each machine, respectively, with resolution of 1250 time points. The waveforms recorded consider only unidirectional variation of the magnetic field.

The first waveform was obtained from the simulations of a machine supplied by a relatively low electrical frequency, which equals 80 Hz. The electrical frequency of the second machine is 525 Hz. Two flux waveforms for the high-frequency machine were chosen in such a way that a maximal magnetic induction value $B_{\max}$ of 1.2 and 1.6 T, respectively, was reached. To validate the results, these waveforms were enforced in an Epstein frame and the losses were measured for the non-sinusoidal waveforms.

A. Loss Prediction for Low-Frequency Non-Sinusoidal Waveform

Fig. 13 presents the time variation and harmonic content of the magnetic induction over one electrical period of the low-frequency machine (80 Hz). The waveform was obtained based on the FE simulation of the machine model. The acquisition of the waveform takes place in the yoke of the stator core of the machine.

The measured value of iron losses under sinusoidal flux condition equals 4.227 W/kg ($B_{\max} = 1.552$ T). The measured loss under non-sinusoidal waveform is equal to 4.265 W/kg. The higher harmonics result in a 0.9% increase of iron losses.

Table II presents the iron losses predicted by the three loss models for the non-sinusoidal waveform from Fig. 13. All three models underestimate the total iron loss value.

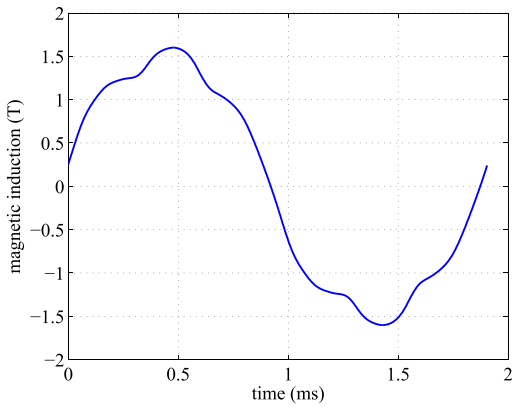

(a)

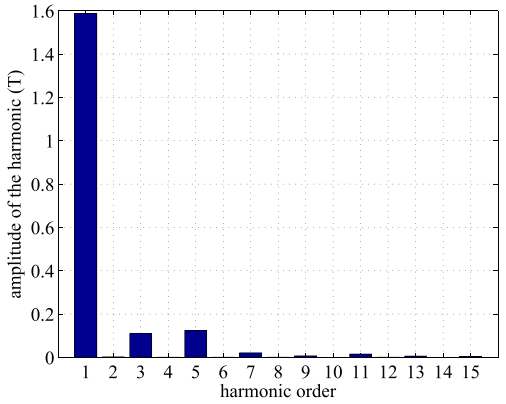

(b)

Fig. 15. (a) Magnetic induction waveform recorded in stator core of the high-frequency machine (525 Hz, $B_{\max} = 1.6$ T). Simulation time is one electrical period of the machine. (b) Harmonic content of the waveform.

B. Loss Prediction for High-Frequency Non-Sinusoidal Waveforms

Figs. 14 and 15 present the time variation and harmonic content of the magnetic induction over one electrical period of the high frequency machine (525 Hz). The waveforms were obtained based on the FE simulation of the electrical machine. Two magnetic induction waveforms were chosen in such a way to represent a maximal magnetic induction $B_{\max}$ of 1.2 (Fig. 14) and 1.6 T (Fig. 15).

The measured loss value for the sinusoidal flux with $B_{\max} = 1.2$ T and 525 Hz equals 32.159 W/kg, whereas the measured value for the non-sinusoidal waveform presented in Fig. 14 is equal to 36.377 W/kg. The increase of iron losses caused by the higher harmonics is equal to 13%.

The accuracy of the simple model 2 for this waveform has a similar range of error in the loss estimation as the frequency model 1 and the time domain model 3. The results of the iron loss estimations with the use of the three models is presented in Table III. Notice, however, that models 1 and 3 overestimate the total value of losses, whereas model 2 underestimates the losses.

Similar observations can be made based on the analysis of Figs. 15 as well as Tables III and IV.

When comparing the correspondence of predicted iron losses to measured ones for the magnetic induction waveforms with two frequencies it can be observed that, the loss models 1 and 3 underestimate the losses for the low-frequency waveform and overestimate for the high frequency. This can be also observed on Figs. 4 and 5.

TABLE III

ERROR BETWEEN THE IRON LOSS VALUE ESTIMATED BY THE THREE LOSS MODELS AND THE MEASURED VALUE OF LOSSES FOR THE HIGH-FREQUENCY WAVEFORM WITH A $B_{\max} = 1.2$ T. LOSSES IN W/kg

	model 1 (frequency)		model 2 (frequency)	model 3 (time)
tot. loss	32.134*	39.364	33.863	38.360
hyst. loss	10.630*	10.630	11.205	10.630
class. loss	12.575*	17.376	12.575	17.320
exc. loss	8.929*	11.358	10.083	10.411
error	11.67%*	-8.21%	6.91%	-5.45%

* losses calculated for fundamental f, where $B_p = B_{max}$.

TABLE IV

ERROR BETWEEN THE IRON LOSS VALUE ESTIMATED BY THE THREE LOSS MODELS AND THE MEASURED VALUE OF LOSSES FOR THE HIGH-FREQUENCY WAVEFORM WITH A $B_{\max} = 1.6$ T. LOSSES IN W/kg

	model 1 (frequency)		model 2 (frequency)	model 3 (time)
tot. loss	59.494*	66.199	58.588	65.244
hyst. loss	20.269*	20.269	19.591	20.269
class. loss	22.386*	26.939	22.385	26.797
exc. loss	16.840*	18.991	16.613	18.179
error	10.77%*	0.72%	12.13%	2.15%

* losses calculated for fundamental f, where $B_p = B_{max}$.

It can be concluded that the simple frequency loss model may not be suitable for the iron loss estimation in the electromagnetic devices, such as electrical machines, due to high errors introduced when the time waveform of magnetic induction contains high value of harmonics.

Both frequency domain model (model 1) considering the effect of higher harmonics on dynamic losses in the steel, and the time domain model (model 3) proved to reliably predict losses even for non-sinusoidal magnetic induction waveform. The errors introduced by these models with respect to measurements did not exceed 9% for all the waveforms considered in this paper.

VI. CONCLUSION

It can be concluded that by simplifying the iron loss model, as in model 2, a large error in loss estimation can be introduced. In addition, it is clear that models 1 and 3 correspond very well with measurements for the sinusoidal flux.

The fitting of the parameters n_0 and V_0 for the modeling of the excess losses in the frequency domain was performed on the basis of measurements of the iron losses under sinusoidal flux conditions for a large range of induction levels and frequencies.

It was shown that the modeled excess losses using the fitted parameter values for equations derived from sinusoidal waveforms correspond well with the ones segregated from measurements under sinusoidal flux conditions regardless the modeling method used (frequency or time domain model).

It can be concluded that by approximating the dependence of n_0 and V_0 on the magnetic induction level by a constant or linear function is introducing an error in modeling the excess losses, when compared with the ones segregated from measurements. The approximation by a linear function introduces a smaller error than in the case of an approximation by a constant.

For the estimation of iron losses for non-sinusoidal waveforms, both frequency, which considering harmonics (Fourier analysis) and time domain models can be used with rather high accuracy.

REFERENCES

[1] G. Bertotti, *Hysteresis in Magnetism, for Physicists, Material Scientists, and Engineers*. San Diego, CA, USA: Academic, 1998.

[2] F. Fiorillo and A. Novikov, "An improved approach to power losses in magnetic laminations under nonsinusoidal induction waveform," *IEEE Trans. Magn.*, vol. 26, no. 5, pp. 2904–2910, Sep. 1990.

[3] E. Barbisio, F. Fiorillo, and C. Ragusa, "Predicting loss in magnetic steels under arbitrary induction waveform and with minor hysteresis loops," *IEEE Trans. Magn.*, vol. 40, no. 4, pp. 1810–1819, Jul. 2004.

[4] G. Bertotti, "Physical interpretation of eddy current losses in ferromagnetic materials. II. Analysis of experimental results," *J. Appl. Phys.*, vol. 57, no. 6, pp. 2110–2126, 1985.

[5] D. Kowal, P. Sergeant, L. Dupré, and A. Van den Bossche, "Comparison of nonoriented and grain-oriented material in an axial flux permanent-magnet machine," *IEEE Trans. Magn.*, vol. 46, no. 2, pp. 279–285, Feb. 2010.

[6] K. Yamazaki and N. Fukushima, "Iron-loss modeling for rotating machines: Comparison between Bertotti's three-term expression and 3-D eddy-current analysis," *IEEE Trans. Magn.*, vol. 46, no. 8, pp. 3121–3124, Aug. 2010.

[7] A. M. Knight, J. C. Salmon, and J. Ewanchuk, "Integration of a first order eddy current approximation with 2D FEA for prediction of PWM harmonic losses in electrical machines," *IEEE Trans. Magn.*, vol. 49, no. 5, pp. 1957–1960, May 2013.

[8] L. R. Dupré, G. Bertotti, and J. A. A. Melkebeek, "Dynamic Preisach model and energy dissipation in soft magnetic materials," *IEEE Trans. Magn.*, vol. 34, no. 4, pp. 1168–1170, Jul. 1998.

[9] L. Dupré, G. Bertotti, V. Basso, F. Fiorillo, and J. Melkebeek, "Generalisation of the dynamic Preisach model toward grain oriented Fe–Si alloys," *Phys. B*, vol. 275, nos. 1–3, pp. 202–206, 2000.

[10] B. Gaussens *et al.*, "Uni- and bidirectional flux variation loci method for analytical prediction of iron losses in doubly-salient field-excited switched-flux machines," *IEEE Trans. Magn.*, vol. 49, no. 7, pp. 4100–4103, Jul. 2013.

[11] A. Belahcen, P. Rasilo, and A. Arkkio, "Segregation of iron losses from rotational field measurements and application to electrical machine," *IEEE Trans. Magn.*, vol. 50, no. 2, pp. 893–896, Feb. 2014.